Electronic Supplementary Information for

A Facile Route to Well-dispersed Ru Nanoparticles-Embedded Self-Templated Mesoporous Carbons for High-Performance Supercapacitors

M. Aftabuzzaman,[a] Chang Ki Kim,[a] Tomasz Kowalewski,[b] Krzysztof Matyjaszewski[b]

and Hwan Kyu Kim[a,*]

[a] *Global GET-Future Lab. & Department of Advanced Materials Chemistry, Korea University, 2511 Sejong-ro, Sejong 339–700, Korea, E-mails: hkk777@korea.ac.kr*

[b] *Department of Chemistry, Carnegie Mellon University, 4400 Fifth Avenue, Pittsburgh, Pennsylvania 15213, USA.*

*To whom correspondence should be addressed: Email: *hkk777@korea.ac.kr*

Table S1. Polymer and ruthenium precursor contents in different composite materials.

Entry	PBA-b-PAN polymer (gm)	$Ru(acac)_3$ (gm)	$Ru(acac)_3$ in polymer (wt%)	Denoted sample	
				Before carbonization	After carbonization
1	2	0.10	4.76	$Ru(acac)_3$@Polymer-1	Ru-NPs@STMC–1
2	2	0.50	20	$Ru(acac)_3$@Polymer-2	Ru-NPs@STMC–2
3	2	0.85	30	$Ru(acac)_3$ Polymer-3	Ru-NPs@STMC–3

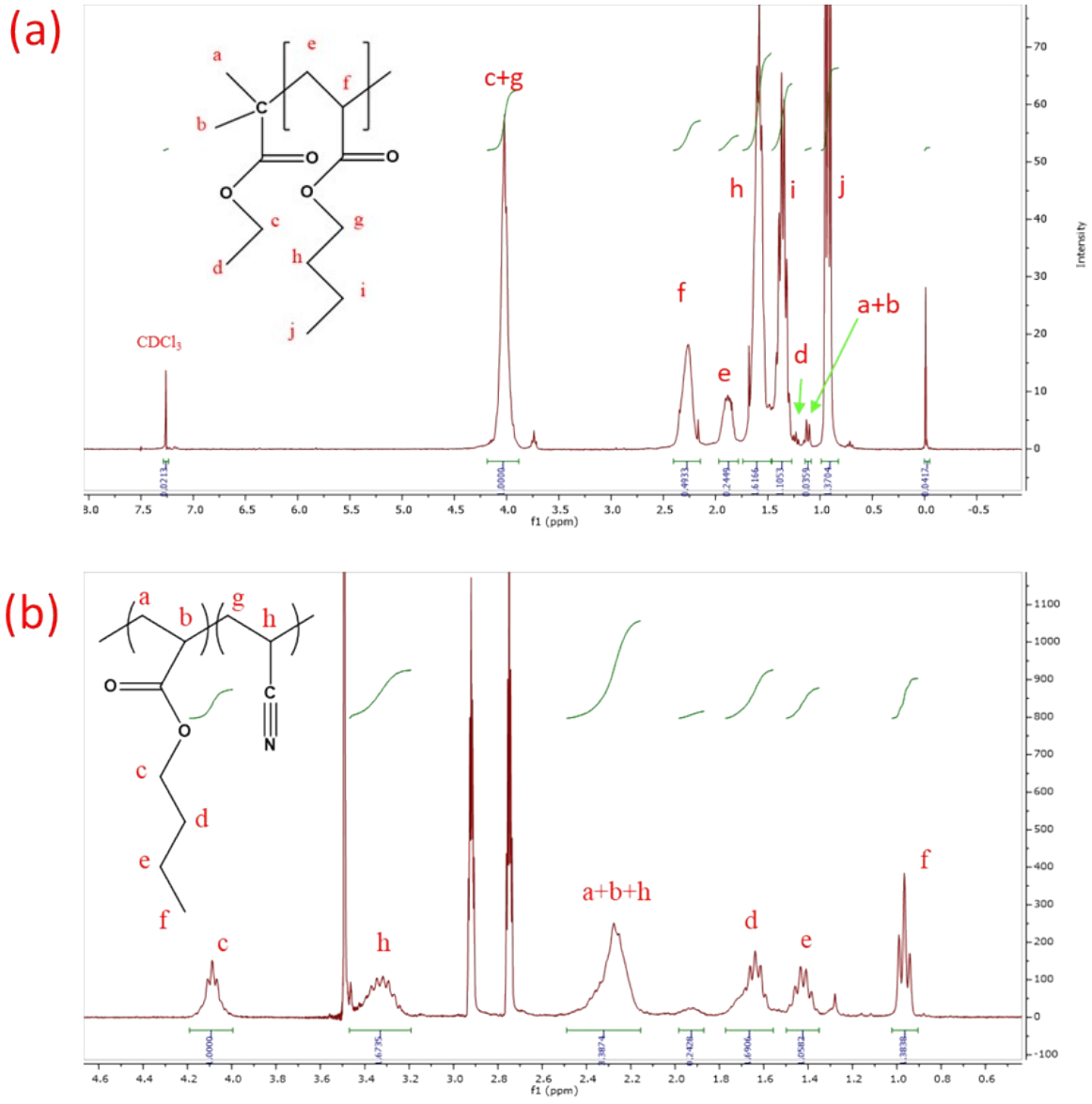

Fig. S1. ^{1}H NMR spectra of (a) PBA-Br macro initiator in $CDCl_3$ solvent, and (b) PBA-b-PAN block copolymer in DMF solvent.

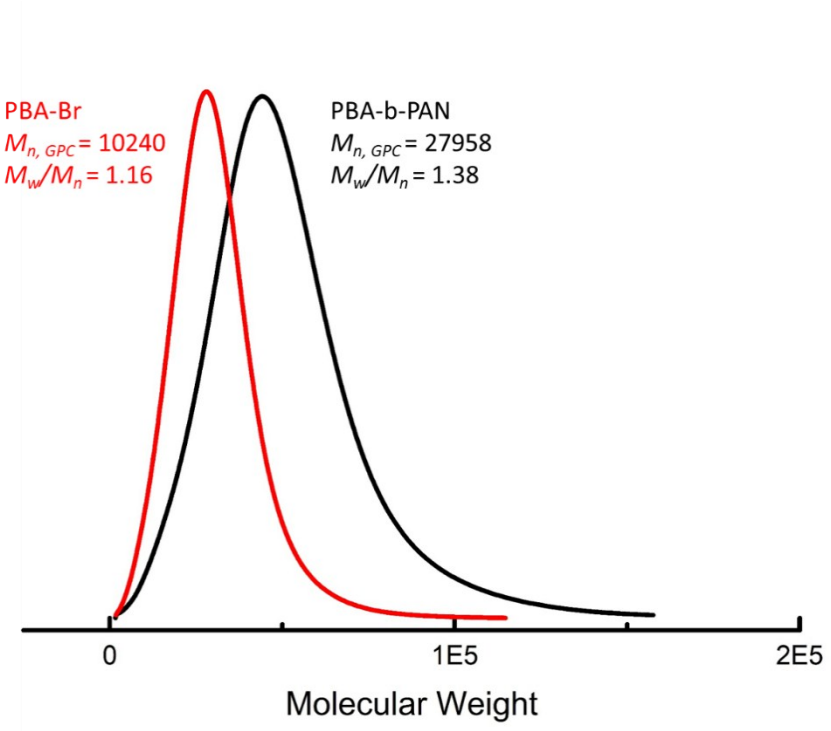

Fig. S2. GPC traces of (a) PBA-Br macro initiator, and (b) PBA-b-PAN block copolymer; increasing molecular weight indicates the successful chain extension of PBA-Br macro initiator.

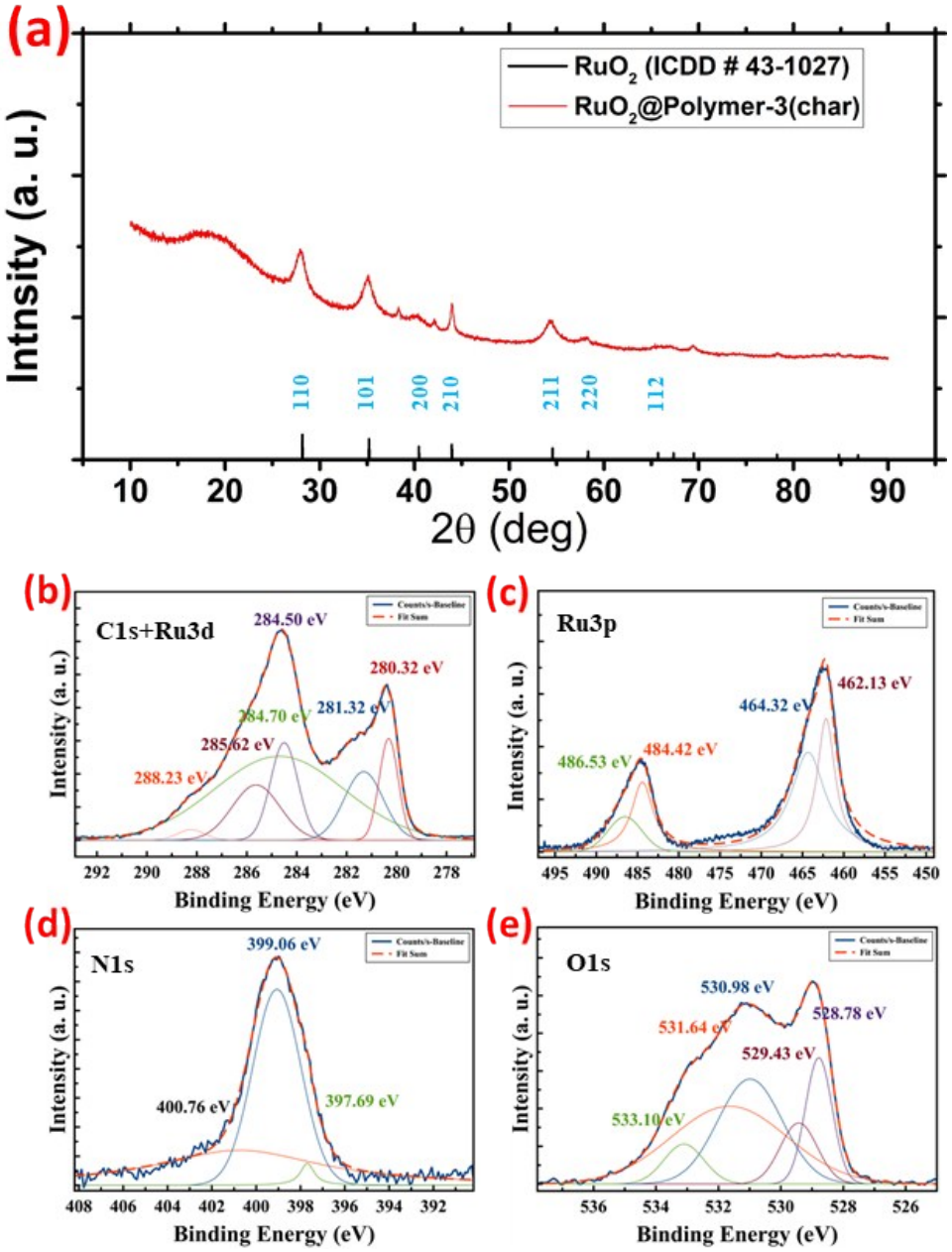

Fig. S3. (a) XRD of RuO_2@Polymer-3 (char, at 280 °C), (b-e) High-resolution deconvoluted XPS spectra of C1s+Ru3d, Ru3p, N1s and O1s of RuO_2@Polymer-3 (char).

The formation of N-doped graphitic carbon from polyacrylonitrile is well known. In the stabilization step at 280 °C cyclization occurred and a six-member hexagonal structure is formed with –C=N–C bond.[48] However, when $Ru(acac)_3$ is added to the PBA-b-PAN polymer, new types

of bond could be formed upon heating. XRD and XPS spectroscopy are used to analyze to explain structure and bonding nature in the composite char. **Fig. S3a** shows the XRD spectra of RuO_2@Polymer-3 (char), which was produced from $Ru(acac)_3$@Polymer-3 at 280 °C in the presence of air. The diffraction peaks at 28.16°, 35.2°, 40.46°, 43.94°, 54.58°, 58.32°, and 65.72° are corresponding to (110), (101), (200), (210), (211), (220) and (112) lattice planes of rutile RuO_2 (**ICDD #43-1027**). **Fig. S3b** shows deconvoluted XPS spectra of C1s+Ru3d. Two peaks at 280.32 and 281.32 eV are assigned to Ru(II)–O/N/C and O–Ru(IV)–O bonds, respectively. Among the other four peaks, three peaks at 284.50, 284.70 and 288.23 eV correspond to the –C–C/–C=C, –C–N/–C=N/–C≡N, and C–O–R/–C=O bonds, respectively, in the carbon matrix and another peak at 285.62 eV is attributed to the $3d_{3/2}$ splitting orbital of Ru(II)–O/N/C or O–Ru(IV)–O bond. However, as C1s and Ru3d overlap in the same spectral region, it is very difficult to identify the oxidation state of ruthenium. That is a reason why it is indispensable to analyses the Ru3p spectra to get clear information about the oxidation state of Ru and bond types. High-resolution deconvoluted XPS spectra of Ru3p show four peaks in **Fig. S3c**; two peaks around 484.42 and 462.13 eV can be assigned to two splitting orbitals, $3p_{1/2}$ and $3p_{3/2}$ of Ru(II)–O/N/C bonds, respectively. Other two peaks around 464.32 and 486.53 eV are assigned to splitting orbital $3p_{1/2}$ and $3p_{3/2}$ of O–Ru(IV)–O bond, respectively. Deconvolution of N1s spectra shows three peaks; the peak at 397.69 eV corresponds to pyridinic-N in C–N=C bond, the peak at 399.06 eV corresponds to C–N–H, N≡C– and non-pyridinic-N in C–N=C bond and the peak at 400.76eV corresponds to coordinated C–N→Ru bond, as shown in **Fig. S3d**. The high-resolution spectra of O1s deconvoluted into five peaks are shown in **Fig. S3e**: two peaks at 529.43 and 528.78eV attributed to C–O–Ru and Ru–O–Ru, other three peaks at 533.10, 531.64, and 530.98 corresponding to –O–H, –C–O and –C=O bonds, respectively. XRD and

XPS data confirm that RuO_2 is formed during the stabilization step of $Ru(acac)_3$@Polymer, and embedded on the polymer char through the C–O–Ru, or coordinated N→Ru–O bond.

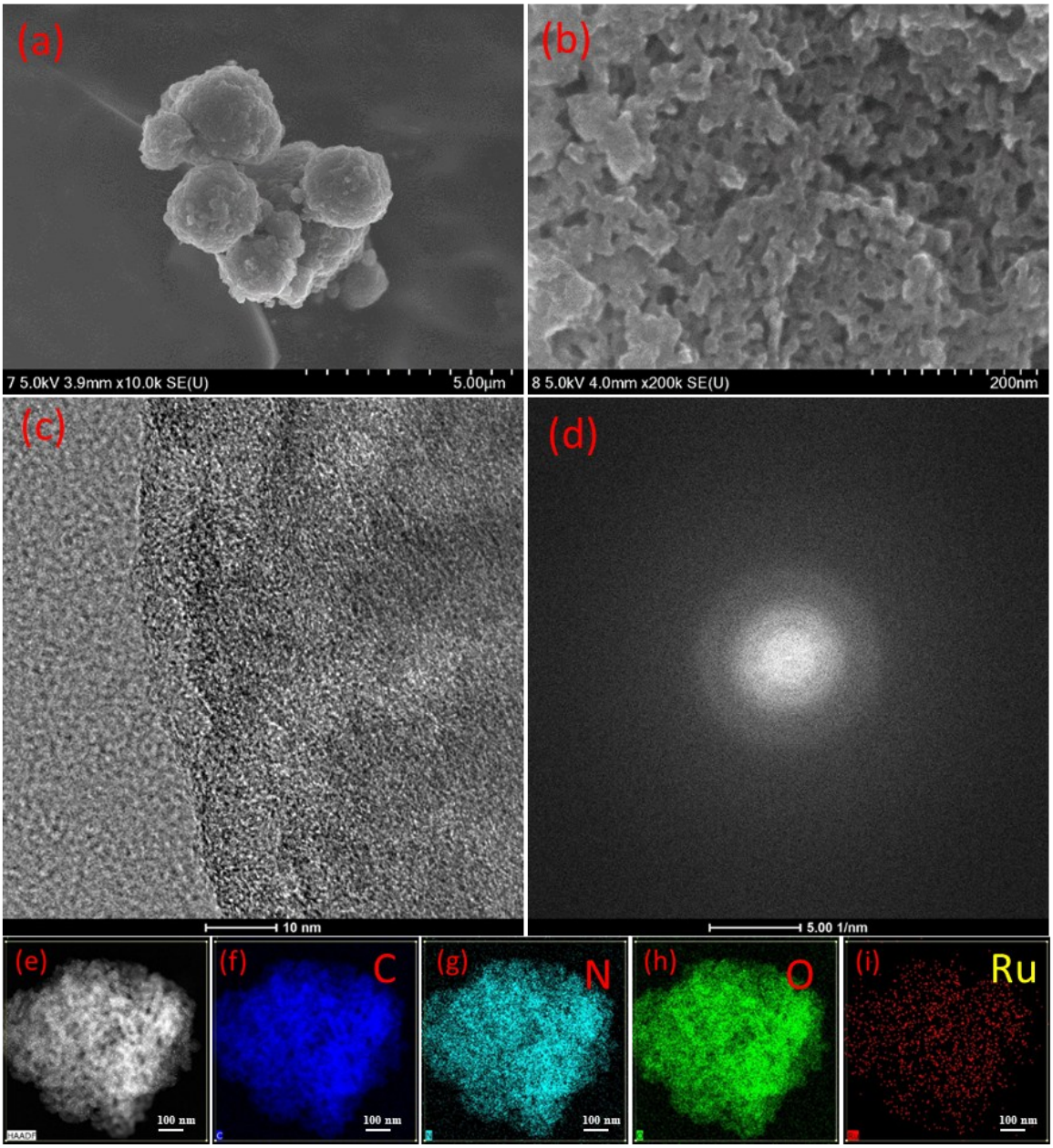

Fig. S4. (a, b) SEM, (c) TEM images at low and high magnification, (d) SAED pattern, and (e–i) TEM HAADF image and corresponding TEM-EDS elemental mapping of Ru-NPs@STMC–1.

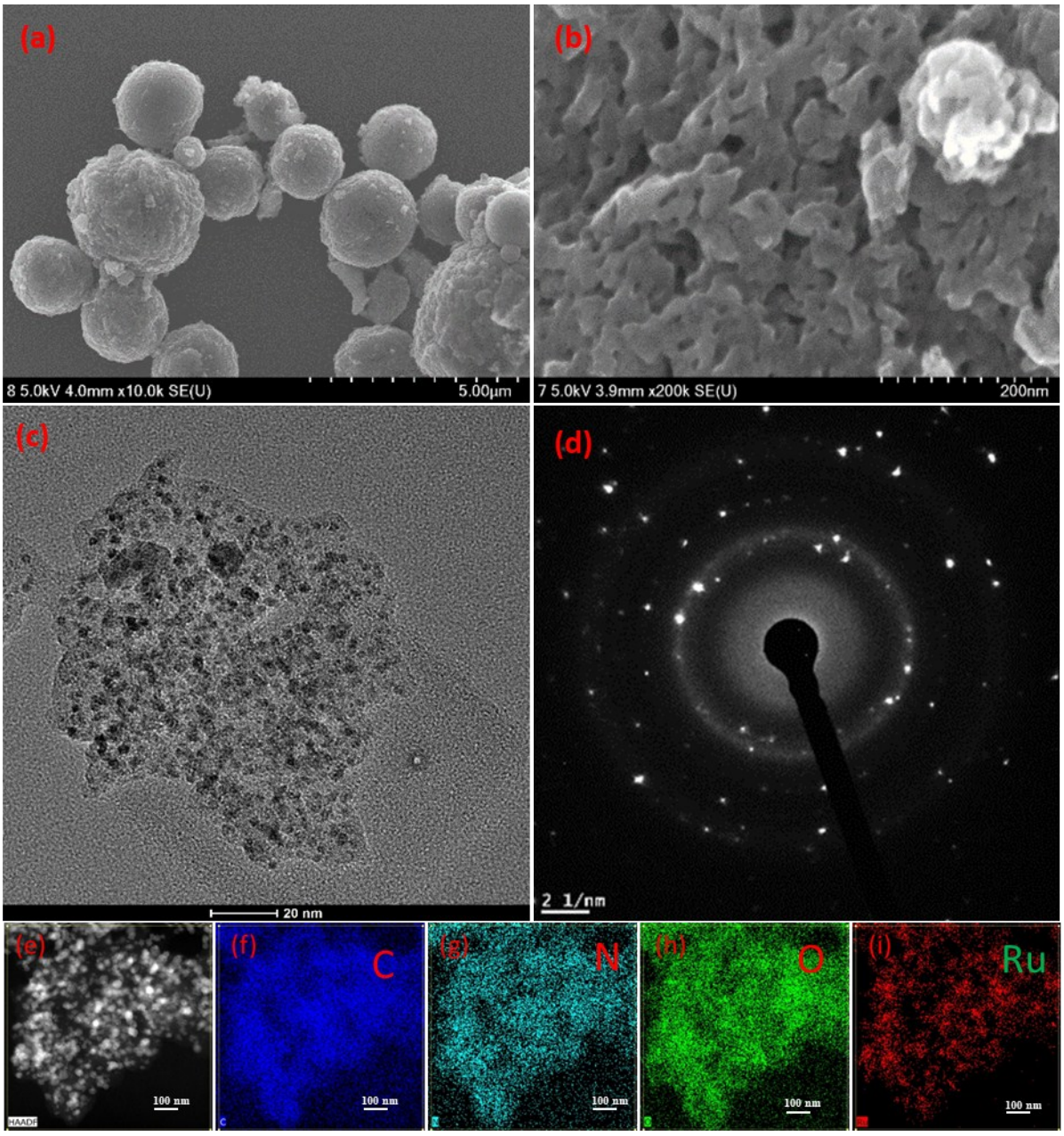

Fig. S5. (a, b) SEM, (c) TEM images at low and high magnification, (d) SAED pattern, and (e–i) HAADF image and corresponding TEM-EDS elemental mapping of Ru-NPs@STMC–2.

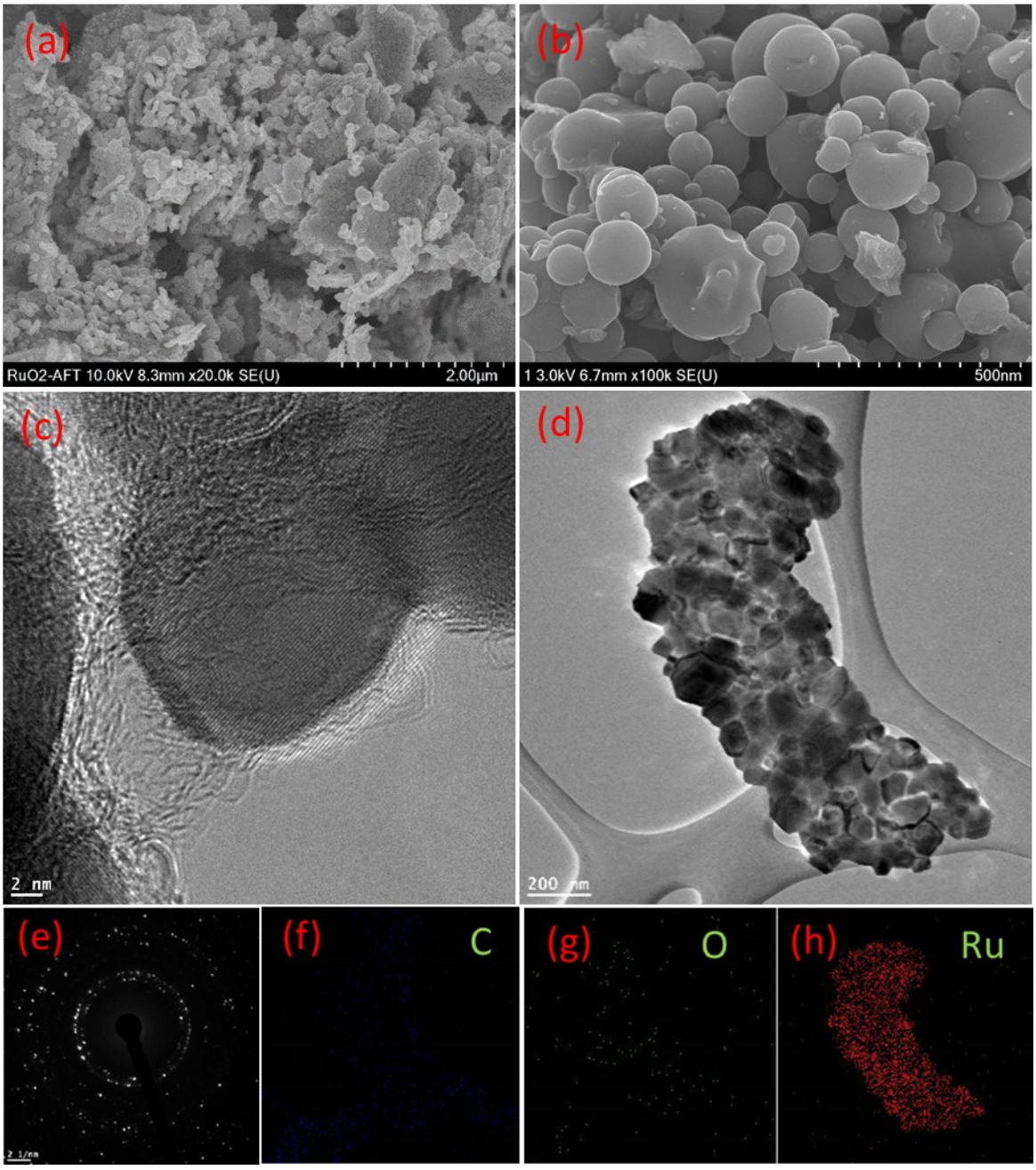

Fig. S6. (a, b) SEM, (c–d) TEM images at low and high magnification, (e) SAED pattern, and (f–h) TEM-EDS elemental mapping of Ru-NPs.

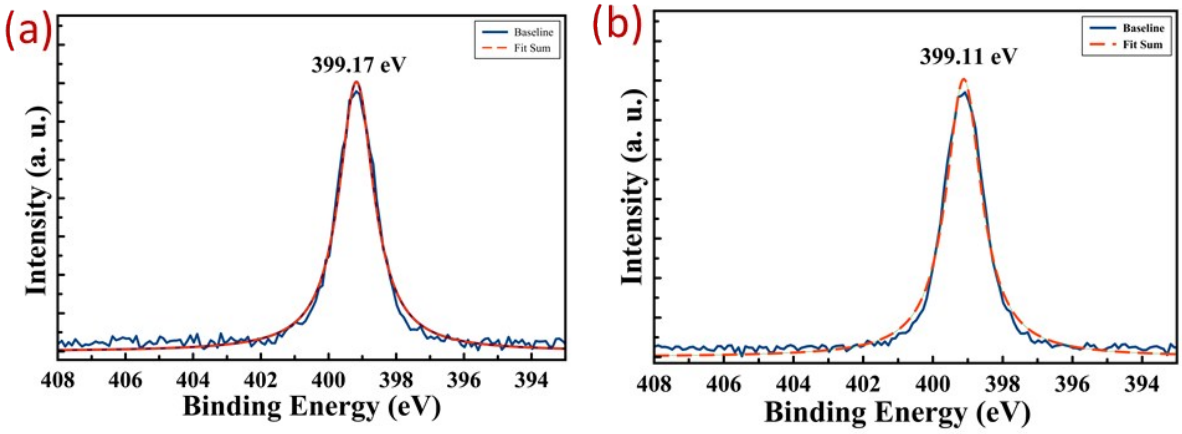

Fig. S7. High-resolution XPS spectrum of N1s of (a) Polymer and (b) $Ru(acac)_3$@Polymer-3.

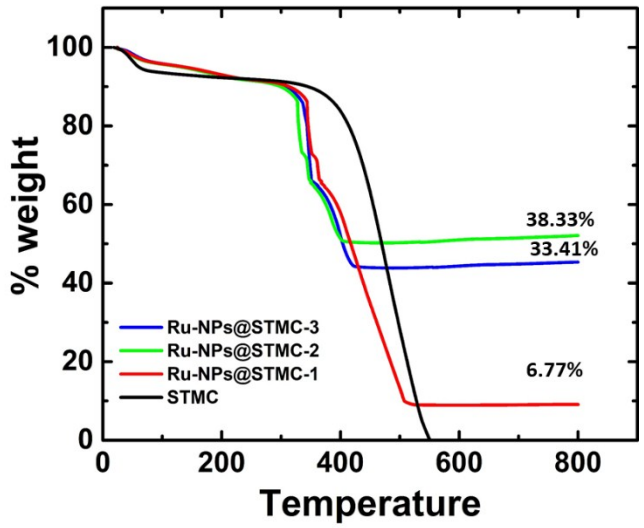

Fig. S8. TGA curves of STMC and Ru-NPs@STMC–*x* at a heating rate of 10 °C min^{-1}.

The weight percent of Ru in the Ru-NPs@STMC–*x* composite was estimated by TGA, as shown in **Fig. S8**. Around 5% weight loss observed below 100 °C is due to the evaporation of adsorbed water. The carbon in the composite is combusted ($C + O_2 \rightarrow CO_2$) and the metallic Ru is oxidized to RuO_2 ($Ru + O_2 \rightarrow RuO_2$) with increasing temperature in the presence of air. The combustion reaction leads to weight loss, whereas the oxidation reaction results in weight increase. The TGA curve is almost stable from 100 to 300 °C, possibly due to the balancing out of the two processes. The rapid weight loss from 300 to 560 °C could be caused by the rapid combustion reaction of carbon. After combustion of all the carbon, the weight gain between 560 and 800 °C could be from the oxidation of metallic Ru to RuO_2. Assuming that only RuO_2 would remain after the TGA test, the Ru content in the composite could be estimated according to the following **equation**:[2]

$$Ru(wt\%) = \frac{\frac{m_2}{M_{RuO_2}} \times M_{Ru}}{m_1} \times 100\% \qquad (S1)$$

where the m_1 is the mass at 300 °C, m_2 the mass at 800 °C, and M_{Ru} and M_{RuO2} are the molar masses of Ru and RuO_2, respectively.

Table S2. Elemental composition of samples measured by different methods.

Samples	Elements	XPS(at%)	EDS(at%)	Elemental Analysis (wt%)
STMC	C	86.67	88.1	83.8
	N	6.7	6.01	8.08
	O	6.63	5.89	11.12
Ru-NPs@STMC–1	C	88.08	89.5	81.64
	N	3.63	3.50	4.89
	O	8.29	6.8	12.29
	Ru	0.17	0.2	1.18
Ru-NPs@STMC–2	C	81.89	85.39	49.38
	N	3.5	3.38	3.93
	O	11.71	8.13	13.4
	Ru	2.9	3.1	33.29
Ru-NPs@STMC–3	C	77.32	75.42	41.89
	N	3.14	3.19	3.02
	O	14.22	14.00	15.21
	Ru	5.32	7.39	39.88

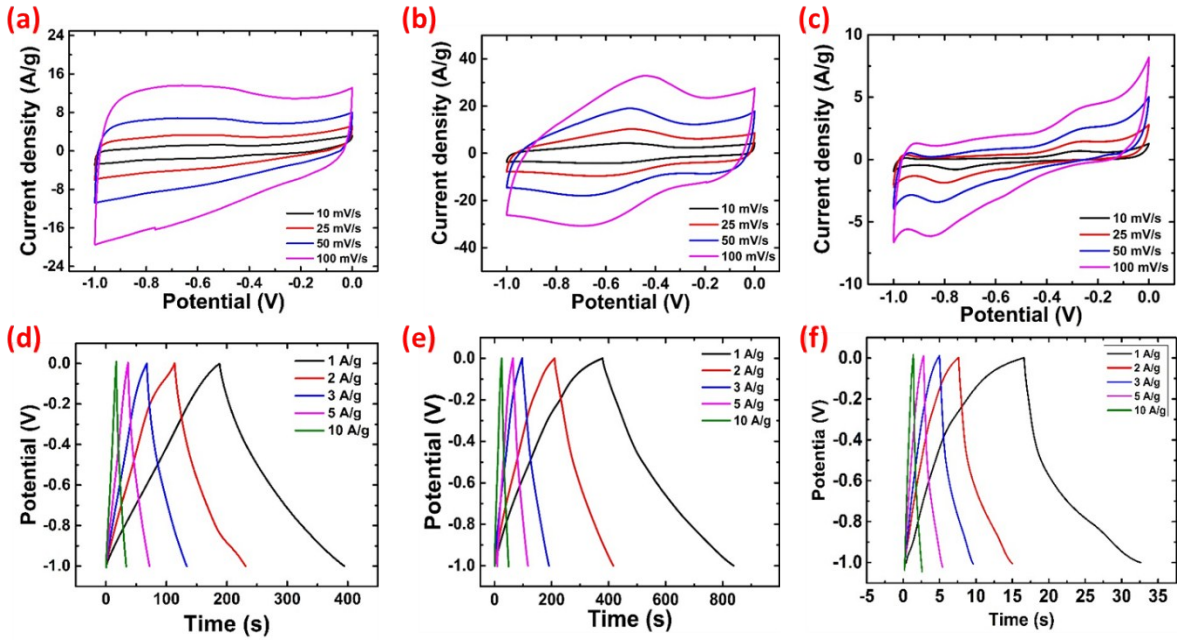

Fig. S9. (a–c) CV and (d–f) GCD curves at different scan rates and current densities, respectively, of Ru-NPs@STMC–1, Ru-NPs@STMC–1 and Ru-NPs@STMC–2.

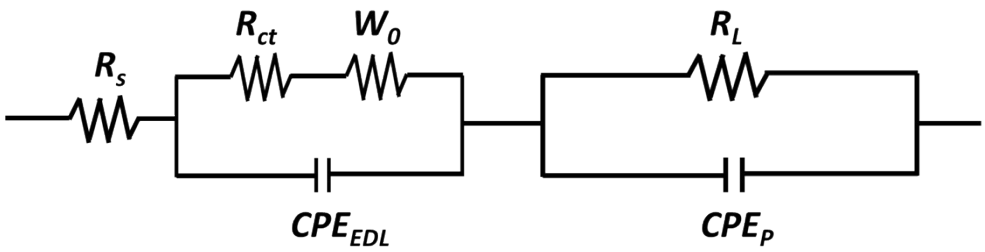

Fig. S10. Equivalent Randles circuit model used to fitting the Nyquist plots. R_S is the equivalent series resistance (ESR), R_{CT} is the charge transfer resistance, R_L is the leakage resistance, $CPEE_{DL}$ is the constant phase element of double layers, CPE_P is the constant phase element of pseudocapacitance, and W_0 is the Warburg element.

Table S3. Equivalent circuit elements obtained by fitting Nyquist plots using the equivalent Randles circuit.

Electrode	R_S (Ω)	R_{CT} (Ω)	W_0			CPE_{EDL} (F)	n	R_L (Ω)	CPE_P (F)	n
			W_0-R (Ω)	W_0-T (s)	n					
STMC	0.29	0.21	2.65×10-7	9.34×10^{-9}	0.44	7.74×10^{-4}	0.88	0.90	0.58	0.40
Ru-NPs@STMC-1	0.29	0.12	1.06×10^{-8}	1.13×10^{-8}	0.47	3.97×10^{-4}	0.97	3.29	1.10	0.38
Ru-NPs@STMC-2	0.30	0.09	1.42×10^{-8}	8.27×10^{-9}	0.45	9.65×10^{-4}	0.95	0.25	1.21	0.42
Ru-NPs@STMC-3	0.30	0.07	9.49×10^{-8}	1.16×10^{-9}	0.48	1.27×10^{-3}	0.97	0.40	1.31	0.35
Ru-NPs	0.30	0.06	5.23	0.06	0.41	4.85×10^{-3}	0.83	0.56	0.05	0.56

Enhanced specific capacitances by the synergetic effect of STMC and Ru-NPs in Ru-NPs@STMC–*x* were calculated using **equations S2** and **S3**:

$$C_m^{syn} = C_m^{\exp} - C_m^{cal} \qquad (S2)$$

$$C_m^{cal} = C_{STMC}(1-x) + C_{Ru}x \qquad (S3)$$

where C_m^{syn}, C_m^{cal} and C_m^{exp} are the enhanced specific capacitance due to synergetic effect, calculated specific capacitance and experimental specific capacitance, respectively. C_{STMC} and C_{Ru} are the experimental capacitances of STMC and Ru-NPs, respectively, and *x* is the weight percentage of Ru in the carbon matrix.

Table S4. Comparison of reported Ru/RuO_2-carbon composite (reference numbers are the same as those in the main text).

Electrode	Wt % of Ru	Electrolytes	Voltage window (V)	Specific gravimetric capacitance (F/g)	References
Ru-NPs@STMC	**38.33**	**6 M KOH**	−1.0–0.0	**656.25 @ 10 mV/s 562.80 @ 1 A/g**	**This work**
Ru/MOC	1.0–1.5	1 M H_2SO_4	0.0–0.8	291 @ 1 A/g	70
Ru/Carbon	14.0	30 wt % H_2SO_4	0.0–1.0	256 @ 1 A/g	67
Ru/RGO	25%	1 M $NaNO_3$	0.0–0.9	270 @ 5.0 mV/s	71
Ru/carbon	60	1 M H_2SO_4	0.0–0.8	549 @ 50 mV/s	69
RuO_2/MC	29.6	1 M H_2SO_4	0.0–1.0	402 @ 1 A/g	55
RuO_2/HGO	42.5	1 M H_2SO_4	0.0–1.0	693 @ 2 mV/s	56
RuO_2/Mxene	-	1 M H_2SO_4	0.0–0.9	388 @ 10 mV/s	24
RuO_2/RCQD	41.9	1 M H_2SO_4	0.0–1.0	594 @ 1 A/g	57
RuO_2/GSC	38.3	1 M H_2SO_4	−0.2–0.8	570 @ 1 mV/s	81
RuO_2/CAC	9.0	3 M KOH	0.0–1.0	510 @ 1 A/g	82
RuO_2/Graphene and CNT hybrid	-	2 MLi_2SO_4	0.0–1.5	502.78 @ 1 A/g	83

Supplementary Reference

[1] T. Kowalewski, M. Zhong, J. F. Whitacre, M. Jaroniec, E. K. Kim, J. P. McGann, K. Matyjaszewski, S.-E. Chun, *J. Am. Chem. Soc.* **2012**, *134*, 14846.

[2] W. Ren, H.-M. Cheng, J. Zhao, G. Zhou, F. Li, D.-W. Wang, Z.-S. Wu, *Adv. Funct. Mater.* **2010**, *20*, 3595.